

# Electronic transport in a series of multiple arbitrary tunnel junctions

U. E. Volmar\*, U. Weber, R. Houbertz and U. Hartmann

*Institute of Experimental Physics, University of Saarbrücken,*

*P.O. Box 151150, D-66041 Saarbrücken, Germany*

(February 1, 2008)

## Abstract

Monte Carlo simulations and an analytical approach within the framework of a semiclassical model are presented which permit the determination of Coulomb blockade and single electron charging effects for multiple tunnel junctions coupled in series. The Coulomb gap in the  $I(V)$  curves can be expressed as a simple function of the capacitances in the series. Furthermore, the magnitude of the differential conductivity at current onset is calculated in terms of the model. The results are discussed with respect to the number of junctions.

PACS: 73.40.Gk, 73.23.Hk

Keywords: Coulomb blockade, Coulomb staircase, Single electron tunneling,  
semiclassical model, multiple tunnel junctions, I-V characteristics

Typeset using REVTeX

---

\*Corresponding author. E-mail: u.volmar@rz.uni-sb.de

Since the development of quantum mechanics, electron tunneling has been widely investigated experimentally [1,2] and extensively discussed in theory. [3,4] The first experiments were performed on metal-insulator-metal (MIM) sandwiches, [1] which permitted the study of tunneling phenomena and the direct correlation of such effects with the thickness of the potential barrier. There are two main theoretical approaches commonly used to describe tunneling phenomena. The first entails solving the time-independent Schrödinger equation and matching the wave functions. [3] However, an exact matching of the wave functions can only be achieved in a one-dimensional approximation. The second method is known as the transfer-Hamiltonian approach, [4] which generally involves a time-dependent Schrödinger equation in the second quantization formalism. In this approach, tunneling of the electrons between the two electrodes is described using a transfer Hamiltonian in addition to the Hamiltonians of the unperturbed electrodes.

For small-scaled systems a particular tunneling phenomenon referred to as single electron tunneling (SET) [5] can occur. SET may be observed, for example, in a system of two electrodes separated by a thin insulating layer, in which a third electrode (e.g., a small metal particle) is embedded. The current through the system is controlled by a single electron if  $k_B T \ll e^2 / [2(C_1 + C_2)]$ , with  $C_1$  and  $C_2$  being the capacitances of the two junctions. A tunneling event therefore changes the total charge of the center electrode by  $\pm e$ , depending on the direction of tunneling, and thus the electrostatic energy of the system. At zero temperature, tunneling is completely prohibited for  $|V| < e / [2(C_1 + C_2)] = \Delta V_{\text{gap}} / 2$  (Coulomb blockade), and the transport process is dominated by charging effects. This means, in particular, that an increase in voltage applied to the double junction system leads to incremental charging, which might manifest itself as steps in the  $I(V)$  characteristic (Coulomb staircase). [5] Such  $I(V)$  characteristics are usually measured at temperatures below 4 K [7] for certain relations of  $R_i C_i$ , such as  $R_1 C_1 \ll R_2 C_2$  ( $R_i$  and  $C_i$  are the tunnel resistance and capacitance of the  $i$ -th junction). The theory developed so far only considers this low-temperature limit.

One important point in understanding SET is the extension of the theory to multiple

tunnel junctions as well as to room temperature. Increasing the temperature to room temperature demands capacitances as small as  $C \simeq 0.1$  aF, since only then does the electrostatic energy of charging by a single electron,  $e^2/2C$ , exceed the thermal energy  $k_B T$ . Nowadays, such capacitances can be realized using small particles [7] or clusters [8] with dimensions in the 1 to 10 nm range.

Here, a theoretical study of  $I(V)$  characteristics of one-dimensional chains of small capacitors coupled in series is presented. Such arrangements can be realized, for example, in granular films of small metal islands or with clusters. An analytical approach for zero temperature in the framework of a semiclassical model is used to explain several features arising in Monte Carlo simulations at finite temperatures. It is shown that the width of the Coulomb gap is directly related to the number of capacitors in the series. An expression is given for calculating the voltages at which steps in the  $I(V)$  characteristic occur. Additionally, the differential conductivity at the current onset just beyond the Coulomb gap is calculated.

Figure 1 shows a system of  $N$  tunnel junctions coupled in series. In the semiclassical model, the state of each tunnel junction is characterized by the voltage drop across [Fig. 1 (a)]. The individual junction voltages can be calculated using Kirchhoff's law together with Gauss's law. Due to tunneling there might be additional electrons on the center electrodes. The voltage  $V_k$  across the  $k$ -th junction with  $n_j$  extra electrons on the  $j$ -th electrode and an externally applied voltage  $V$  can be written as

$$V_k(\dots n_j \dots, V) = \frac{1}{C_k} \left( \frac{C_1 V - C_1 e \sum_{m=2}^N \left( 1/C_m \sum_{j=1}^{m-1} n_j \right)}{1 + C_1 \sum_{m=2}^N 1/C_m} + e \sum_{j=1}^{k-1} n_j \right), \quad (1)$$

where  $C_m$  denotes the capacitance of the  $m$ -th tunnel junction.  $V_k$  causes a mutual shift in the Fermi energies of the electrodes.

The tunneling rates across the junctions, which can be calculated using Fermi's golden rule, are given by the following expression (for tunneling through the  $k$ -th junction from right to left):

$$r_k = \int_{-\infty}^{+\infty} dE \frac{2\pi}{\hbar} |T(E)|^2 D_{k-1}(E - E_{k-1}) f(E - E_{k-1}) D_k(E - E_k) [1 - f(E - E_k)], \quad (2)$$

where  $f(E)$  is the Fermi-Dirac distribution. If we consider, as usual, the density of states  $D$  near the Fermi level and the tunnel matrix element  $T$  to be energy-independent, that is  $D_k(E - E_k) = D_k^0$  and  $|T(E)|^2 = |T_0|^2$ , the tunneling rates from right to left ( $r_k$ ) and reverse ( $l_k$ ) [cf. Fig.1(b)] are

$$r_k(\dots n_j \dots, V) = \frac{1}{e^2 R_k} \frac{\Delta E_k^{\leftarrow}}{1 - \exp(-\Delta E_k^{\leftarrow}/k_B T)} \quad (3)$$

and

$$l_k(\dots n_j \dots, V) = \frac{1}{e^2 R_k} \frac{\Delta E_k^{\rightarrow}}{1 - \exp(-\Delta E_k^{\rightarrow}/k_B T)}, \quad (4)$$

where the tunneling resistances  $R_k$  are given by  $1/R_k = (2\pi e^2/\hbar) D_{k-1}^0 D_k^0 |T_0|^2$ . The energy that an electron gains by tunneling through the  $k$ -th junction,  $\Delta E_k^{\leftarrow}$  or  $\Delta E_k^{\rightarrow}$ , may be calculated by integrating the difference between the neighboring Fermi levels over the tunneling event:

$$\left. \begin{array}{l} \Delta E_k^{\leftarrow} \\ \Delta E_k^{\rightarrow} \end{array} \right\} = -e \int_0^{\pm 1} dq V_k(\dots, n_{k-1} - q, n_k + q, \dots, V). \quad (5)$$

This is just the change in the electrostatic energy of the  $k$ -th capacitor. Evaluating the integral leads to a simple expression for the energy changes:

$$\left. \begin{array}{l} \Delta E_k^{\leftarrow} \\ \Delta E_k^{\rightarrow} \end{array} \right\} = \mp e V_k(\dots n_j \dots, V) \frac{e^2}{2} \frac{C_1}{C_k^2 (1 + C_1 \sum_{m=2}^N 1/C_m)} - \frac{e^2}{2C_k}. \quad (6)$$

The  $I(V)$  characteristics of this system can be determined numerically by Monte Carlo simulation. One main feature of the results which arises in the simulations is a widening of the Coulomb gap with increasing number of tunnel junctions (Fig.2). This can be understood for the zero-temperature limit of the system. Also, the differential conductivity at current onset (see inset of Fig.3) can be calculated in this limit. For  $T = 0$ , a tunneling event is impossible whenever a tunneling electron would lose energy, that is  $\Delta E_k^{\leftarrow} < 0$  or  $\Delta E_k^{\rightarrow} < 0$ , respectively. From any state defined by the numbers  $n_j$  of extra electrons on the center

electrodes, the system may undergo a number of transitions by tunneling of an electron somewhere in the series. The energy changes associated with these transitions,  $\Delta E_k^{\leftarrow}$  and  $\Delta E_k^{\rightarrow}$ , are directly related to the applied voltage via Eq.(6). In the simplest case of only one extra electron in the series (or one extra hole, i.e., the absence of one electron), these energy differences are negative for zero voltage, i.e., tunneling is impossible. An increasing voltage causes the energies to increase towards and then above zero, thus increasing the number of possible tunneling events. The energy differences associated with tunneling through the terminating junctions of the chain are the last to become positive. Therefore, the Coulomb gap of multiple junction systems can be determined by examining the voltages at which either  $\Delta E_1^{\rightarrow}$  and  $\Delta E_1^{\leftarrow}$  or  $\Delta E_N^{\rightarrow}$  and  $\Delta E_N^{\leftarrow}$  cross zero. For  $C_1 < C_N$ , the first tunnel junction is the one that dominates the process and the Coulomb gap is found to be

$$\Delta V_{\text{gap}} = e \sum_{i=2}^N \frac{1}{C_i} \quad (7)$$

For  $C_1 > C_N$ , the last junction dominates the process, which means that the sum in Eq.(7) runs from  $i = 1$  to  $N - 1$ . A similar approach to calculate the size of the Coulomb gap was chosen before, [9] although the system of junctions is not as general as that considered here (the capacitances are taken to be all equal).

Higher threshold voltages can in principle be determined in a similar manner, thus accounting for the structure of multiple junction  $I(V)$  curves. Using a fairly simple computer program, one can calculate the states that are accessible from the “ground state”, which is given by  $n_j = 0$  for all  $j$ ’s, and one can determine the threshold voltages at which new states become accessible. A state is accessible if a sequence of tunneling events with nonvanishing probability leads to it. These threshold voltages provide an intuitive understanding of the steps in the  $I(V)$  characteristic as well as an exact prediction of the voltages at which they occur. Until now, the step structures in such simulations have usually been presented without explanation or simply been characterized as unusual. [10,11] In the present analysis, however, the number of predicted threshold voltages exceeds the number of steps that occur in the numerical simulation. The occurrence of steps depends crucially on the choice of the

resistance values, as will be discussed subsequently.

Just beyond the Coulomb gap, i.e., at voltages slightly above the first threshold voltage  $V_{\text{th}} = \frac{1}{2}\Delta V_{\text{gap}}$ , the most probable process is one electron (hole) tunneling through the whole chain of junctions before the next electron (hole) enters. The average time that the electron spends on one particle of the chain is given by the inverse tunneling rate. The average time  $\tau$  to tunnel through the whole chain is therefore

$$\tau = \frac{1}{l_N(0, \dots, 0, V)} + \frac{1}{l_{N-1}(0, \dots, 0, 1, V)} + \dots + \frac{1}{l_1(1, 0, \dots, 0, V)}. \quad (8)$$

This time  $\tau$  is valid for voltages  $V$  slightly above the threshold voltage:  $V = V_{\text{th}} + \delta V$ , where  $\delta V$  is small. At zero temperature, the tunneling rates  $l_k$  are given by the expression

$$l_k(\dots n_j \dots, V) = \begin{cases} 0 & \text{for } \Delta E_k^{\rightarrow} < 0, \\ \Delta E_k^{\rightarrow} / (e^2 R_k) & \text{for } \Delta E_k^{\rightarrow} \geq 0. \end{cases} \quad (9)$$

Therefore, just above the threshold voltage  $V_{\text{th}}$ , the voltage at which the energy change at the  $N$ th junction,

$$\Delta E_N^{\rightarrow} = \frac{e}{C_N \sum_{m=1}^N 1/C_m} \delta V,$$

crosses zero, the first term in Eq.(8) dominates. The  $I(V)$  dependence near  $V_{\text{th}}$  is thus given by

$$I(V) = \frac{e}{\tau} = e l_N(0, \dots, 0, V) = \begin{cases} 0 & \text{for } V < V_{\text{th}}, \\ (C_N R_N \sum_{m=1}^N 1/C_m)^{-1} \delta V & \text{for } V \geq V_{\text{th}}. \end{cases} \quad (10)$$

In the inset of Fig.3, Monte Carlo results obtained close to the first threshold voltage are shown for two sets of parameters and are compared with the asymptotes given by Eq.(10). This figure demonstrates how drastically the differential conductivities at current onset, given the same average slope of  $1/\sum_{i=1}^N R_i$ , depend on the value of the resistance of junction 1, which in this case determines the threshold voltage. It also shows the good agreement of the numerical data with the analytical result.

In a more rigorous approach, probabilities  $P(\dots n_j \dots)$  must be assigned to the states  $(\dots n_j \dots)$  of the system. These probabilities must be solutions of the stationary master equation of the system. The correct expansion for the stationary current is then given by

$$I = e \sum_{\text{all } (\dots n_j \dots)} P(\dots n_j \dots) [l_N(\dots n_j \dots, V) - r_N(\dots n_j \dots, V)], \quad (11)$$

summing over all possible electronic states  $(\dots n_j \dots)$  of the system with an arbitrary number of extra electrons on the center electrodes.

For voltages  $V = V_{\text{th}} + \delta V$  near the first threshold voltage, the probability of the “ground state”  $(0, \dots, 0)$  is almost 1, i.e.,  $P(0, \dots, 0) \simeq 1$ , and the probabilities of all other states are negligible. This results from the fact that, while the transition rates from the state  $(0, \dots, 0)$  to neighboring states are zero or nearly zero, the transition rates back to the ground state are already finite. Furthermore,  $r_N(0, \dots, 0, V)$  vanishes for positive voltages  $V$ , leaving only  $l_N(0, \dots, 0, V)$ . Therefore Eq.(11) reduces to

$$I = e l_N(0, \dots, 0, V) \quad (12)$$

near the first threshold voltage, which is the same result as obtained above in Eq.(10).

It is, of course, quite difficult to calculate analytically the probabilities of the states from the full master equation of the system, although it is possible (for capacitances all equal) to write an analytical expression for the average current without an explicit solution of the master equation in the case when the voltage corresponds to the first two steps in the  $I(V)$  characteristic. [12] Qualitatively, one can expect — as at the first threshold voltage — the steepest steps in  $I(V)$  to occur when tunneling through the junction with the lowest resistance value creates access to a new state. Higher steps may only occur when the associated threshold voltage is determined by a junction  $k_0$  for which

$$(C_{k_0} R_{k_0} \sum_{m=1}^N 1/C_m)^{-1} \gg \frac{1}{\sum_{i=1}^N R_i}.$$

This tendency can also be seen in the results of Fig.3. The solid arrows indicate voltages at which new states become accessible by tunneling through junction 1, which manifests itself

as steps in the (thicker)  $I(V)$  curve for parameter set 1 ( $R_1$  small). At voltages indicated by the dashed arrows, new states become accessible by tunneling through the last junction 6, corresponding to steps in the (thinner) curve for parameter set 2 ( $R_6$  small).

In conclusion, Monte Carlo simulations of  $I(V)$  characteristics in a one-dimensional arrangement of tunnel junctions as well as an analytical approach have been presented. The analytical results may be used to understand the features found in the simulations. The results are in general useful for the qualitative and quantitative understanding of experimental  $I(V)$  curves. The voltages at which steps occur can be predicted using the presented formalism — in particular, the size of the Coulomb gap can be determined. Efforts are currently in progress to extend the theoretical approach to finite temperatures and to investigate in more detail the influence of certain system parameters, such as the resistance values in the junction array, on the resulting  $I(V)$  curves.

#### ACKNOWLEDGMENTS

This work was supported by BMBF (Grant: 13N6562).



## REFERENCES

- [1] I. Giaever, Science **183**, 1253 (1974).
- [2] See, e.g., R. Wiesendanger and H. Güntherodt (eds.), *Scanning tunneling microscopy I*, Springer Series in Surface Science **29**, (Springer, Berlin, 1990).
- [3] J. G. Simmons, J. Appl. Phys. **34**, 1793 (1963).
- [4] J. Bardeen, Phys. Rev. Lett. **6**, 57 (1968).
- [5] D. V. Averin and K. K. Likharev, J. Low Temp. Phys. **62**, 345 (1986).
- [6] D. V. Averin, A. N. Korotkov, and K. K. Likharev, Phys. Rev. B **44**, 6199 (1991).
- [7] J. G. A. Dubois, E. N. G. Verheijen, J. W. Gerritsen, and H. van Kempen, Phys. Rev. B **48**, 11260 (1993).
- [8] G. Schmid, Chem. Rev. **92**, 1709 (1992).
- [9] B. Laikhtman, Phys. Rev. B **41**, 138 (1990); N. S. Bakhvalov, G. S. Kazacha, K. K. Likharev, and S. I. Serdyukova, Zh. Eksp. Teor. Fiz. **95**, 1010 (1989) [Sov. Phys. JETP **68**, 581 (1989)].
- [10] E. Bar-Sadeh, Y. Goldstein, C. Zhang, H. Deng, B. Abeles, O. Millo, Phys. Rev. B **50**, 8961 (1994).
- [11] M. Amman, E. Ben-Jacob, and K. Mullen, Phys. Lett. **A142**, 431 (1989).
- [12] A. Korotkov, Phys. Rev. B **50**, 17674 (1994).

## FIGURES

FIG. 1. (a) Circuit diagram of a system of  $N$  tunnel junctions in series, represented by their capacitances  $C_i$ . The voltage drop across the  $i$ -th tunnel junction is  $V_i$ . (b) Schematic diagram of the tunnel junctions coupled in series, showing the various tunneling rates  $l_i, r_i$ .

FIG. 2. Monte Carlo simulations of  $I(V)$  curves for (a) 3, (b) 5 and (c) 10 tunnel junctions. The parameters for the simulations are  $C_1 = 1.2$  aF,  $C_2 = \dots = C_{N-1} = 1.4$  aF,  $C_N = 2.8$  aF and  $R_1 = 0.01$  M $\Omega$ ,  $R_2 = \dots = R_{N-1} = 280$  M $\Omega$ ,  $R_N = 2.8$  M $\Omega$  and  $T = 4.2$  K.

FIG. 3. Monte Carlo simulation and analytical predictions for the  $I(V)$  step structure of a 6-junction system. The parameters are  $T = 0.01$  K,  $C_1 = 1.2$  aF,  $C_{2\dots5} = 2.8$  aF,  $C_6 = 4.4$  aF (in both cases),  $R_1 = 24$  M $\Omega$ ,  $R_{2\dots5} = 560$  M $\Omega$ ,  $R_6 = 8000$  M $\Omega$  (thick line, set 1) and  $R_1 = 8000$  M $\Omega$ ,  $R_{2\dots5} = 560$  M $\Omega$ ,  $R_6 = 24$  M $\Omega$  (thin line, set 2). Solid arrows indicate access through junction 1, dashed arrows through junction 6 (see text). In the inset, current onsets for the two sets of parameters are magnified. The diamonds (set 1) and squares (set 2) are Monte Carlo results, whereas the solid lines display the asymptotes for  $V \rightarrow V_{\text{th}}$  from the analytical expression. The dot-dashed line shows the average slope for reference.

Fig.1: U.E.Volmar et al., Electronic transport in a series ...

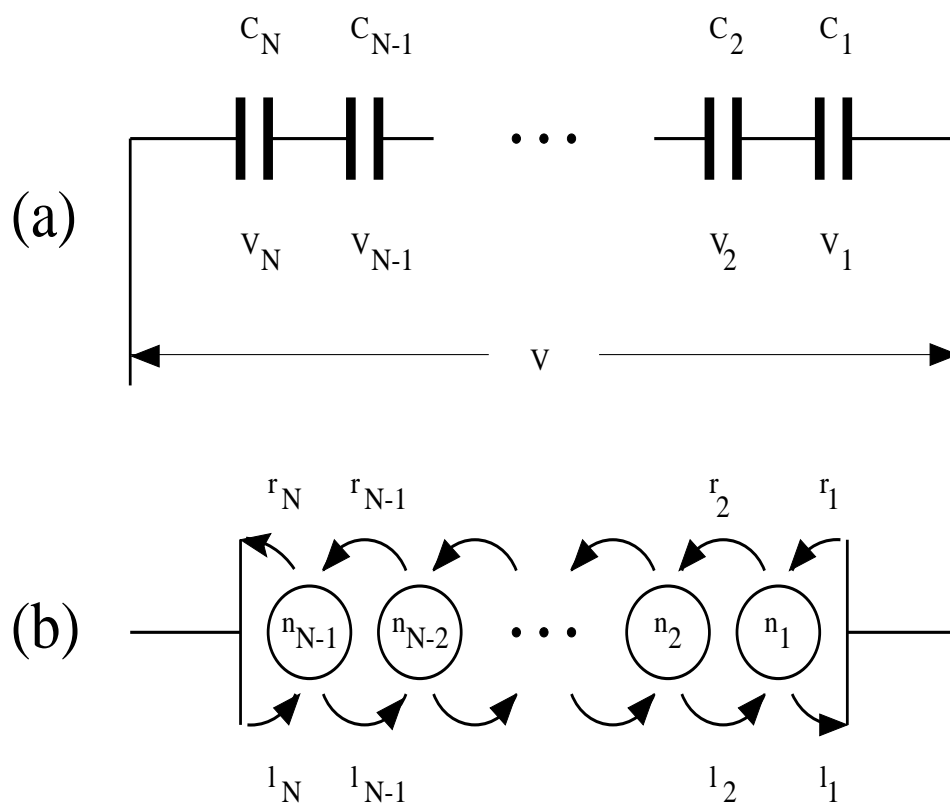


Fig.2: U.E.Volmar et al.,Electronic transport in a series ...

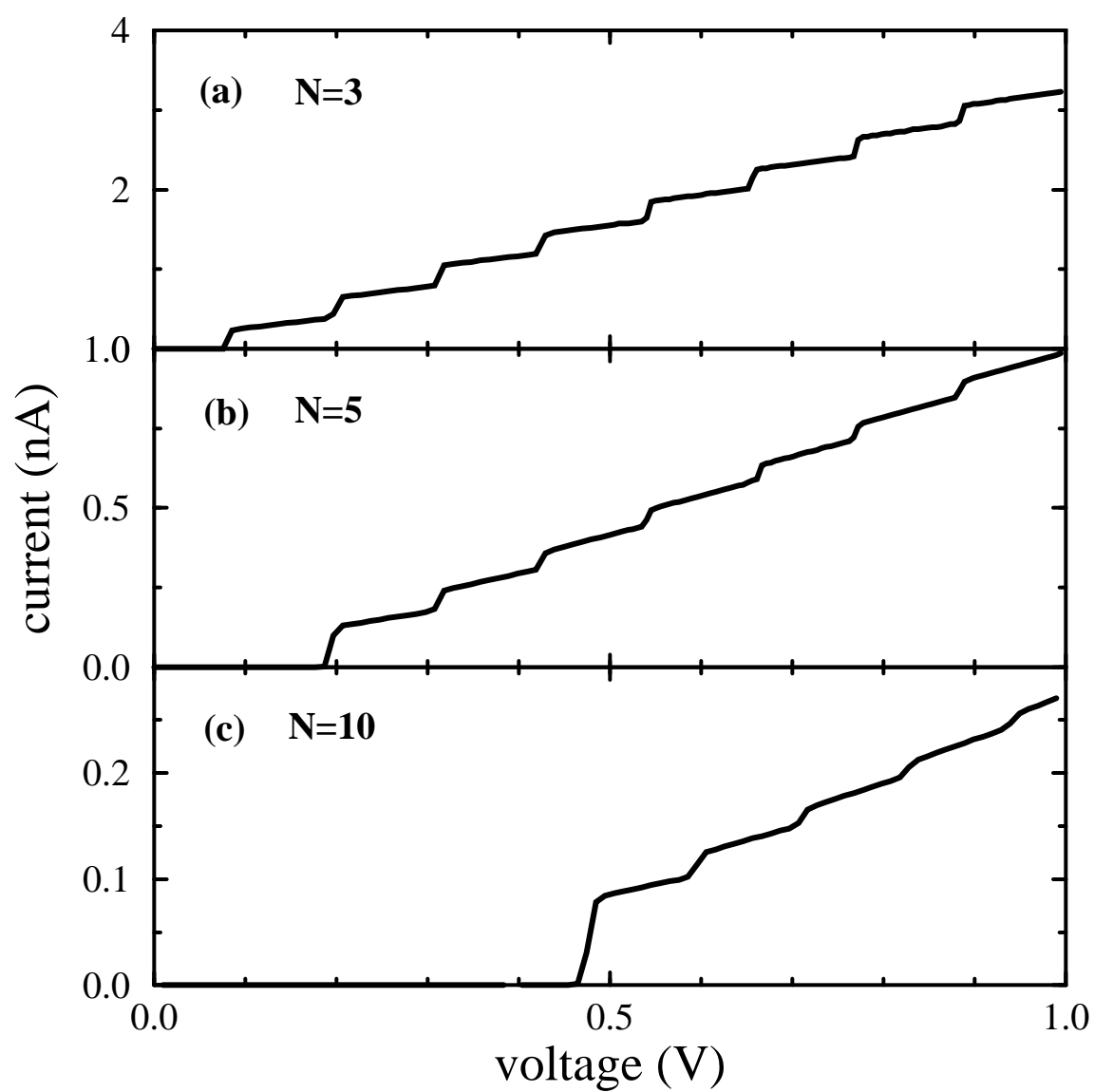


Fig.3: U.E.Volmar et al.,Electronic transport in a series ...

